

## Field and laboratory experiments on high dissolution rates of limestone in stream flow

著者	Hattanji Tsuyoshi, Ueda Mariko, Song Wonsuh, Ishii Nobuyuki, Hayakawa Yuichi S., Takaya Yasuhiko, Matsukura Yukinori
journal or publication title	Geomorphology
volume	204
page range	485-492
year	2014-01
権利	(C) 2013 Elsevier B.V. NOTICE: this is the author's version of a work that was accepted for publication in Geomorphology. Changes resulting from the publishing process, such as peer review, editing, corrections, structural formatting, and other quality control mechanisms may not be reflected in this document. Changes may have been made to this work since it was submitted for publication. A definitive version was subsequently published in Geomorphology, 204, 2014. <a href="http://dx.doi.org/10.1016/j.geomorph.2013.08.027">http://dx.doi.org/10.1016/j.geomorph.2013.08.027</a>
URL	<a href="http://hdl.handle.net/2241/120668">http://hdl.handle.net/2241/120668</a>

doi: 10.1016/j.geomorph.2013.08.027

# Field and laboratory experiments on high dissolution rates of limestone in stream flow

Tsuyoshi Hattanji<sup>1</sup>, Mariko Ueda<sup>2</sup>, Wonsuh Song<sup>3</sup>, Nobuyuki Ishii<sup>4</sup>,  
Yuichi S. Hayakawa<sup>3</sup>, Yasuhiko Takaya<sup>3</sup> and Yukinori Matsukura<sup>1</sup>

<sup>1</sup> Faculty of Life and Environmental Sciences, University of Tsukuba

<sup>2</sup> Graduate School of Life and Environmental Sciences, University of Tsukuba

<sup>3</sup> Center for Spatial Information Science, The University of Tokyo

<sup>4</sup> College of Geoscience, University of Tsukuba

## Abstract

Field and laboratory experiments were performed to examine dissolution rates of limestone in stream flow. Field experiments were conducted in three stream sites (A – C) with different lithological or hydrological settings around a limestone plateau in the Abukuma Mts., Japan. Sites A and B are allogenic streams, which flow from non-limestone sources into dolines, and site C has a karst spring source. Tablets made of limestone from the same plateau with a diameter of 3.5 cm and a thickness of 1 cm were placed in the streams for 3 years (2008 – 2011) where alkalinity, pH and major cation concentrations were measured periodically. The saturation indices of calcite (SI<sub>c</sub>) of stream water were  $-2.8 \pm 0.4$  at site A,  $-2.5 \pm 0.4$  at site B and  $-0.5 \pm 0.4$  at site C. Annual weight loss ratio for tablets were extremely high at site A ( $0.11\text{--}0.14 \text{ mg cm}^{-2} \text{ d}^{-1}$ ), high at site B ( $0.05 \text{ mg cm}^{-2} \text{ d}^{-1}$ ), and low at site C ( $0.005 \text{ mg cm}^{-2} \text{ d}^{-1}$ ). The contrasting rates of weight loss are mainly explained by chemical conditions of stream water. In addition, laboratory experiments for dissolution of limestone tablets using a flow-through apparatus revealed that flow conditions around the limestone tablet is another important factor for dissolution in the stream environment. These results revealed that limestone dissolves at a rapid rate where water unsaturated to calcite continuously flows, such as in an allogenic stream.

Key words: Karst, Limestone, Dissolution, Weathering experiment, Tablet, Stream flow

## 29    **1. Introduction**

30    Limestone plateaus with many dolines develop in karst terrains, especially in humid temperate regions such as  
31    Japan. One of the most important factors related to evolution of karst landform is denudation rate in various  
32    environments including ground surface, unsaturated soil, saturated soil and streams.    The shallow weathered  
33    bedrock zone immediately beneath the soil-bedrock interface plays an important role in limestone dissolution  
34    and evolution of karst landforms (Williams, 1983). In typical karst terrains, however, limestone also dissolves  
35    in streams flowing around the margin of the plateau where stream water or groundwater is in direct contact  
36    with limestone. For example, an ‘allogenic stream’, a stream flowing from basins underlain by non-carbonate  
37    rocks, also makes a doline or other karst features (White, 1988; Ford and Williams, 2007). The impact of  
38    allogenic streams on landform evolution has not been well studied.

39    There are several techniques for estimating denudation rates of karst terrains. Chemical denudation rates in  
40    karst areas were classically estimated from Ca flux, i.e. average Ca ion concentrations and annual discharge  
41    from springs (e.g. Smith and Atkinson, 1976). For the case of a doline with an allogenic stream, however,  
42    estimating denudation rate from the Ca flux method has the following problems: (1) allogenic inputs are  
43    mixed with autogenic (on plateau) inputs during flow process in cave, and (2) caves immediately below  
44    dolines with allogenic stream are generally inaccessible.

45    The technique of field weathering experiments using a weight loss approach is an effective method for  
46    estimating the potential for dissolution under various environmental conditions (Trudgill, 1977; Jennings,  
47    1981; Crabtree and Trudgill, 1985; Trudgill et al., 1994; Inkpen, 1995; Urushibara-Yoshino et al., 1999;  
48    Matsukura and Hirose, 1999; Dixon et al., 2001; Thorn et al., 2002, 2006; Plan, 2005; Matsukura et al. 2007;  
49    Yoshimura et al., 2009). The method is simple: installing a rock specimen with a known weight and surface  
50    area to a field site and measuring the weight loss after a period. The method also has problems that (1) the  
51    methodology itself may impact results of weathering rates (Inkpen, 1995) and (2) the estimated denudation  
52    rate for a short-term experiment (a few years) would be affected by temporal variation. However, this method  
53    enables us to directly estimate ‘spatial variation’ of limestone dissolution rate at any site. Past weathering  
54    experiments using this technique have focused on (1) topography (Crabtree and Trudgill, 1985 ; Plan, 2005),  
55    (2) duration (Trudgill et al., 1994), (3) climate (Urushibara et al., 1999), (4) difference between limestone and  
56    other rocks (Matsukura and Hirose, 1999; Thorn et al., 2002, 2006; Plan, 2005; Matsukura et al. 2007), and

57 (5) dissolution in caves (Yoshimura et al., 2009). Most of these experiments were conducted on the ground  
58 surface or in soil, but they did not particularly focus on dissolution in stream flow, including allogenic stream  
59 flow.

60 The present study focuses on the dissolution of limestone in stream flow along a margin of a karst plateau.  
61 The aim of the present study is to determine which environmental factors are significant for the dissolution  
62 under flowing water, based on a combined approach of field and laboratory experiments using limestone  
63 tablets and chemical analysis of the contact water.

64

## 65 **2. Field Experiment**

### 66 *2.1. Study site*

67 Field weathering experiments were conducted around a small karst plateau, ‘Sendaihora’, in the central  
68 Abukuma Mountains, Japan (Fig. 1), located in humid temperate region with humid summers and dry winters.  
69 The mean annual precipitation (1981–2010) at the nearest meteorological station ‘Ono-nimachi’ is 1245 mm,  
70 of which 71% falls from May to October. Mean monthly temperature ranges from −0.9 °C to 22.9 °C and the  
71 annual mean is 10.5 °C. The maximum depth of snow cover around the test sites reaches 20–30 cm in  
72 February. The vegetation around the sites is a combination of natural broad-leaved forest and planted forest of  
73 Japanese cedar, although grassland is artificially maintained around the top of the plateau. The underlying  
74 bedrock of the plateau is recrystallized massive limestone, which is in contact with shale layers at the eastern  
75 side and has a strike in the NNW–SSE direction with almost vertical dip (Ehiro et al., 1989). These  
76 sedimentary rocks are metamorphosed by Cretaceous granite, which outcrops to the southern and eastern  
77 margins. The age of these layers has not been determined precisely. An airborne LiDAR DTM with 2 m  
78 resolution reveals that two major active dolines have developed in a valley along the lithological boundary  
79 between limestone and shale (Fig. 1c). Two headwater streams originating from eastern hillslopes underlain  
80 by shale flow into both dolines, which are also connected to the two major caves beneath the karst plateau  
81 (Marui et al., 2003).

82 (Fig. 1)

83

### 84 *2.2 Methods*

We selected three sites of stream for field experiment (Fig. 2). Sites A and B are headwater streams flowing into the dolines, and site C is located ~30 m downstream of a karst spring (Fig. 1c). Table 1 shows hydrological and geomorphic conditions for the sites. Local channel gradient represents average gradient for a 50-m reach around each stream site. The gradient of site A is almost twice as that of site B. Channel morphology at sites B and C is a 'pool' whereas site A is located in a 'rapid' section. Stream discharge measured with a volumetric method varied from  $90 \text{ cm}^3 \text{ s}^{-1}$  (site C) to  $4900 \text{ cm}^3 \text{ s}^{-1}$  (site B) at base flow stages (average of May 24, June 21, and July 21, 2008). We visually confirmed that these streams are perennial and almost constant base flows continued even in cold, snowy winter season from the start to the end of the field experiment. Although we could not make direct measurements on flow velocity due to shallowness or slowness of the flow, we have estimated mean water flux from stream width, flow depth, and discharge at base flow stage (Table 1). Water flux at site A is about 6.5 cm/s (depth of  $2 \pm 1 \text{ cm}$ ) which is slightly higher than at site B (4.5 cm/s; depth of  $10 \pm 3 \text{ cm}$ ), and much higher than at site C (0.3 cm/s; depth of  $10 \pm 3 \text{ cm}$ ).

(Table 1)

(Fig. 2)

Limestone blocks for field experiment were taken near the Abukuma Cave, Fukushima Prefecture, which is lithologically the same bedrock below the two dolines (sites A and B) and the upstream source of site C. The limestone blocks which were used were uniform. The limestone blocks were cored and then sliced into standard-sized tablets, which have a diameter of 34.5 mm, a thickness of  $11.0 \pm 0.6 \text{ mm}$ , a surface area of  $30.60 \pm 0.37 \text{ cm}^2$ , a weight of  $27.2 \pm 1.2 \text{ g}$  and a bulk density of  $2.67 \pm 0.02 \text{ g cm}^{-3}$ . The density of rock was  $2.78 \pm 0.03 \text{ g cm}^{-3}$ , and therefore, porosity was estimated to be  $3.7 \pm 1.4\%$ . X-ray fluorescence analysis by Suzuki et al. (2000) showed that the limestone contains 55.5% of CaO, 0.22% of MgO, 0.19% of  $\text{Al}_2\text{O}_3$ , and 0.10% of  $\text{FeO} + \text{Fe}_2\text{O}_3$ .

We prepared a total of eight tablets for the field experiment. The surfaces of the tablets were polished with carborundum #400. The tablets were weighed to an accuracy of 1 mg using a microbalance after oven drying at  $110 \text{ }^\circ\text{C}$  for 24 hours. We placed a nylon mesh bag (mesh size of 3.57 mm), in which a set of two tablets were enclosed, at each stream site. The drawstrings of the mesh bags were fixed to tree trunks or branches (Fig. 2). These tablets were collected about every six months and rinsed carefully with water in the laboratory.

113 Then the tablets were dried at 110 °C for 24 hours and reweighed. To evaluate the impacts of washing and  
114 drying on dissolution rate, only washing and drying processes in the laboratory were simultaneously  
115 performed for two ‘control’ tablets during the entire experimental period. The field experiment was conducted  
116 for about 3 years from April 30, 2008 to May 3, 2011. The actual period of installation of tablets in the stream  
117 flow was 1044 days, which is shorter than the whole period (1100 days) because the treatment in laboratory  
118 was required for a total of 56 days. We also confirmed that the tablet bag at site C had moved out of the stream  
119 flow during the last period by May 3, 2011. Therefore, we used the 863-day records until October 10, 2010 for  
120 site C.

121 In order to understand chemical conditions of stream sites related to limestone weathering, we repeated *in situ*  
122 measurement and sampling of stream water for a total of 21 times in the experimental period. The pH of  
123 stream water was measured *in situ* with a portable glass electrode system (Horiba D-54) composed of an  
124 Ag-AgCl internal electrode and 3.33 mol L<sup>-1</sup> KCl solution. The temperature dependence of pH was  
125 compensated automatically. The pH meter was calibrated using three standard solutions within 24 hours  
126 before measurement. Although the system officially has an accuracy of ±0.02 for the observed pH range, the  
127 fluctuation exceeds 0.02 during *in situ* measurement. We recorded a value of pH about 15 – 20 min after the  
128 setting of the glass electrode to achieve a fluctuation of less than 0.05 within 5 min. Stream water was  
129 sampled for alkalinity titration and ICP-AES analysis. Alkalinity was determined by titration to pH 4.8 using  
130 0.01N H<sub>2</sub>SO<sub>4</sub> and BCG-MR indicator using micro-pipettes at a 0.1 mL interval. The remaining original water  
131 sample was filtered to 0.20 µm to measure concentrations of dissolved Ca, Mg, Si, K, and Na ions with  
132 ICP-AES (Nippon Jarrell-Ash ICAP-757 from 2008 to 2010, Perkin Elmer Optima 7300DV from 2010 to  
133 2011) at the Research Facility Center for Science and Technology in University of Tsukuba. The relative  
134 standard deviation for Ca concentration was less than 2% except for two data in site A. We did not analyze  
135 concentrations of other anions. Marui et al. (2003) reported that the stream water at sites A and B contains Cl  
136 of 3 – 5 mg L<sup>-1</sup>, SO<sub>4</sub> of 1 – 4 mg L<sup>-1</sup>, NO<sub>3</sub> of 0 – 0.2 mg L<sup>-1</sup> and PO<sub>4</sub> of 0 – 0.02 mg L<sup>-1</sup> in August, 2001 and  
137 February, 2002. The anion concentrations during the experiment would be at a similar level, since there were  
138 no significant changes in land use and vegetation from 2001 to early 2011. Using all the measured chemical  
139 parameters, we calculated saturation index for calcite (SI<sub>c</sub>), which is defined as logarithmic ratio of the ion  
140 activity product over equilibrium constant for reaction of calcite dissolution (Ford and Williams, 2007). We

used the PHREEQC software with a geochemical database file of phreeqc.dat (ver 2.15.0) for calculation of SIc (Parkhurst and Appelo 1999).

### 2.3. Results

We calculated two weathering rates for tablets: (1) mean rate of weight loss and (2) annual weight loss ratio, (Table 2). The mean rate of weight loss is the total weight loss for each tablet divided by surface area and experimental period, i.e. 1044 days for sites A/B and 863 days for site C. Weight loss of two control tablets revealed that the washing and drying processes cause weight losses of  $1.3 \pm 3.6$  mg per one treatment. The uncertainty for single measurement is about 4 mg. For the entire experimental period, six treatments give a reduction of 7.5 mg, and five treatments (by 863 days at site C) give reduction of 6.3 mg. Therefore, the observed weight loss is reduced by 7.5 mg for sites A and B and by 6.3 mg for site C. The mean daily rate of weight loss varied from  $0.005 \text{ mg cm}^{-2} \text{ d}^{-1}$  at site C (No. 9) to  $0.137 \text{ mg cm}^{-2} \text{ d}^{-1}$  at site A (No. 18) (Table 2). We also calculated annual weight loss ratio in order to compare the results of the other studies. The annual weight loss ratio at site A was extremely high ( $4.5\text{--}5.7\% \text{ a}^{-1}$ ), and exceeded any other annual weight loss ratio reported in previous field experiments using limestone or dolomite tablets:  $0.1\text{--}0.6\% \text{ a}^{-1}$  at Magnesian Limestone hillslopes (Crabtree and Trudgill, 1985; Trudgill et al., 1994),  $0.01\text{--}3.04\% \text{ a}^{-1}$  for dolomite at Kärkevagge (Thorn et al. 2006), and  $0.08\text{--}3.7\% \text{ a}^{-1}$  for the same limestone installed in granitic soil of Abukuma Mountains (Matsukura et al., 2007; see Fig. 1b for location). The surface of tablets at site A had been intensively affected by dissolution. For example, the surface of a tablet (No. 17) placed at site A was more rugged than the tablets placed at site C or non-weathered polished limestone (Fig. 3).

(Table 2)

(Fig. 3)

All the chemical indices such as pH, alkalinity, and Ca concentration were higher at site C and lower at sites A and B (Table 3). Annual average water temperature was almost the same ( $10\text{--}11^\circ\text{C}$ ). Saturation indices for calcite (SIc) were low ( $-3$  to  $-2$ ) at both sites A and B, and high (about  $-0.5$ ) at site C. Fig. 4 shows temporal variation of pH and SIc. These indices of water chemistry have a weak seasonal variation, where both pH and SIc increase in the fall and decrease in spring for all sites. The difference in SIc between sites is clearer than the difference in pH. SIc of the stream water at site C was significantly greater than the other sites because

contrasts in alkalinity and Ca concentration are more obvious (Table 3). Stream water at site C sometimes reached the state of saturation with respect to calcite ( $SI_c \sim 0$ ). In contrast, stream waters at sites A and B were under-saturated ( $< -1$ ) to calcite for the whole period. The observed contrasts between site C and the other sites are explained by lithology of source area (Fig. 1). Stream water at site C originated from a karst spring below the plateau which had already reacted with limestone through percolation into the plateau, while the stream water at site A had no chance to be in contact with limestone in the upstream sources underlain by shale. Although a part of drainage area for site B includes the limestone plateau, site B has a slightly higher pH and  $SI_c$  than site A (Table 3). The partial source of the limestone plateau is not likely to contribute to the water chemistry at site B. The Welch's t-test revealed that the difference of average pH or  $SI_c$  between sites A and B is not statistically significant ( $p > 0.05$ ). Therefore, sites A and B have similar chemical conditions in terms of dissolution of calcite.

(Table 3)

(Fig. 4)

The difference in stream water chemistry, such as  $SI_c$ , affects the mean rate of weight loss, particularly for the case of site C where stream water is sometimes chemically saturated to calcite. However, there is a question that the very high rates of weight loss at sites A and B can be explained by water chemistry alone. There is a significant difference in flow conditions around tablets (Table 1, Fig. 2), and this may also contribute to the difference in dissolution rate for these sites.

### 3. Laboratory experiments

#### 3.1. Experimental Design

A laboratory experiment was carried out to test the effect of flow rate of stream water on dissolution of limestone tablet. We employed a flow-through apparatus (Fig. 5). Distilled water in an input solution bottle was infused into a 60-mL reaction bottle with a peristaltic pump at a constant flow rate, and the solution in the reaction bottle was drained at the same rate simultaneously. This apparatus and a similar style one were also used for an experiment to examine the dissolution of granodiorite tablets (Yokoyama and Matsuskura, 2006), and to test the effect of calcite saturation of stream water on dissolution of limestone tablet (Hattanji et al. 2008). Three runs were conducted for 24 days at the three different flow rates of  $100 \text{ mL d}^{-1}$ ,  $550 \text{ mL d}^{-1}$  and



4500 mL d<sup>-1</sup>. For each run, one limestone tablet was inserted into the reaction bottle. We used the limestone tablets with the same size and origins as those used in the field experiment. The reaction bottle was settled in an incubator to keep the temperature at 20°C. Although the temperature was higher than average stream water temperature (~10°C) at sites A – C, variation of several equilibrium constants ( $pK_1$ ,  $pK_2$ , and  $pK_C$ ) related to the dissolution reaction series of calcite was less than 2% in this temperature range (Ford and Williams, 2007; p.48, Table 3.6). Partial pressure values of CO<sub>2</sub> in laboratory atmosphere were constant at 0.05–0.06%. The output solution drained from the reaction bottle was collected for chemical analysis including measurements of pH, alkalinity and dissolved cation concentrations every two days. The analytical method is almost the same as those in the field experiment. The same portable pH meter (Horiba D-54, an accuracy of ± 0.02) was used for measurement of pH. Alkalinity was determined by titration to pH 4.8 using 0.01N H<sub>2</sub>SO<sub>4</sub> and BCG-MR indicator using micro pipettes at a 0.1 mL interval. The dissolved Ca, Mg, Si, K, and Na ions were measured with ICP-AES (Perkin Elmer Optima 7300DV).

(Fig. 5)

### 3.2. Results

We calculated two parameters representing weathering rates: (1) mean rate of weight loss and (2) dissolution rate of calcite. Again, mean rate of weight loss is total weight loss of each tablet divided by surface area and the experimental period, i.e. 24 days. The daily mean rate of weight loss varied from 0.037 mg cm<sup>-2</sup> d<sup>-1</sup> for run 1 to 0.124 mg cm<sup>-2</sup> d<sup>-1</sup> for run 3 (Table 4). However, duration of laboratory experiment is shorter than that of the field experiment, and therefore total amount of weight loss is much smaller (< 100 mg).

(Table 4)

The second approach calculates ‘dissolution rate of calcite’ based on concentration of Ca ion for input and output solutions. For all the runs, the output solution had higher Ca concentration than its input solution, and loss of Ca from the tablet can be estimated from the increments of Ca concentration. Cumulative loss of Ca from a tablet by the  $n$ th day,  $W_n$  (mg), is:

$$W_n = \sum_{i=1}^n ([Ca^{2+}]_{OUTi} - [Ca^{2+}]_{INi}) \cdot \rho v_i \quad (1)$$

where  $[Ca^{2+}]_{OUTi}$  is concentration of Ca ion in the output solution on the  $i$ th day in ppm (mg kg<sup>-1</sup> solution),

224  $[Ca^{2+}]_{INi}$  is concentration of Ca ion in the input solution on the  $i$ th day in ppm ( $mg\ kg^{-1}$  solution),  $v_i$  is volume  
225 of the output solution on the  $i$ th day in litre, and  $\rho$  is density of solution ( $= 1\ kg\ L^{-1}$ ). We estimated the  
226 dissolution rate of Ca using the slope of regression line for the temporal increase of  $W_n$ . Assuming that all the  
227 increments in the concentration of Ca ion are originated from the dissolution of calcite ( $CaCO_3$ ) on the surface  
228 of limestone tablet, we can convert dissolution rate of Ca into dissolution rate of calcite using weight ratio of  
229 calcite to Ca (100/40). The calculated dissolution rate of calcite per unit surface area ranged from 0.018 to  
230  $0.098\ mg\ cm^{-2}\ d^{-1}$  (Table 4).

231 Both dissolution rate of calcite and mean rate of weight loss increased with increasing flow rate (Fig. 6). This  
232 result indicates that flow rate is a significant controlling factor on dissolution and weathering of limestone  
233 tablet. Although the SIc of output solutions were very low ( $< -3$ ) for all the runs, the solution in the reaction  
234 bottle indicated higher SIc values, ranging from  $-3.5$  to  $-0.61$  (Table 4). For the case of the lowest flow rate  
235 (run 1), the solution remaining in the reaction bottle was not completely saturated but close to saturation (SIc  
236  $= -0.61$ ). The slower flow rate allows development of a thicker boundary layer with higher pH and Ca  
237 concentrations, which, in turn, restricts fast dissolution. For the case of the highest flow rate (run 3) with low  
238 SIc ( $-3.5$ ), faster circulation enhanced the dissolution of tablet.

239 The mean rate of weight loss was  $0.02$ – $0.03\ mg\ cm^{-2}\ d^{-1}$  higher than dissolution rate of calcite calculated from  
240 water chemistry analysis (Fig. 6 and Table 4). The factors responsible for this inconsistency would be: (1) the  
241 effect of physical detachment of vulnerable parts, such as the edge or rough surface, during drying and  
242 weighing process, (2) removal of ‘diffusion boundary layer’ (Ford and Williams, 2007) surrounding the tablet  
243 surface before weighing, which contains more amounts of dissolved Ca, and (3) errors in measurement or  
244 analysis. Accumulation of errors in ICP-AES analysis was only  $0.002\ mg\ cm^{-2}\ d^{-1}$  for the greatest case of run  
245 3. Although the errors in weight measurement ( $\pm 4\ mg$ ) are equivalent to 5–20% of total measured weight loss,  
246 these are much smaller than the systematic difference between two measurements (Fig. 6). These facts imply  
247 that effect of physical detachment and removal of a boundary layer are possible reasons for the inconsistency.  
248 For these cases, mean rate of weight loss would approach the value of ‘dissolution rate of calcite’ if the  
249 laboratory experiment was to continue for a duration as long as the field experiment.

250 (Fig. 6)

251

252

## 253 4. Discussion

### 254 4.1. Field weathering rates vs dissolution rates in the laboratory

255 We compared the results of field experiment with laboratory experiment, in order to understand what controls  
256 the dissolution of limestone in streams around a karst plateau. Rates of weight loss or dissolution rates of  
257 calcite were plotted against saturation indices for calcite (SI<sub>c</sub>, Fig. 7a) or pH (Fig. 7b) of stream water for field  
258 experiment or output solutions for laboratory experiment. For laboratory runs, the SI<sub>c</sub> values for output  
259 solutions were used here as a reference, which represents flowing water outside of the diffusion boundary  
260 layer developed on tablet surface. The results of laboratory experiment by Hattanji et al. (2008) were also  
261 plotted in Fig. 7, in which the effect of calcite saturation of circulating water on limestone dissolution was  
262 tested using the same apparatus and the same-sized limestone tablets. The runs were conducted at a constant  
263 flow rate of  $63 \pm 2 \text{ mL d}^{-1}$  and continued for 23 days with various input solutions with different SI<sub>c</sub>.  
264 Dissolution rate of calcite was similarly calculated using Eq. (1).

265 (Fig. 7)

266 In Fig. 7a, the field rate at site C, which represents a flow from a karst spring, show a good fit with the data of  
267 Hattanji et al. (2008) at the near equilibrium solution. The result ensures that slower rate of weight loss at site  
268 C is well explained by water chemistry, in other words, the near equilibrium state of flowing water. In contrast,  
269 dissolution rates and mean rates of weight loss were scattered for lower SI<sub>c</sub> (−3 to −2). Sites A and B have  
270 about 10 times higher weathering rates of laboratory run 1 or the data of Hattanji et al. (2008), even under  
271 similar chemical conditions of flowing water.

272 Dissolution rates vary from  $0.018 \text{ mg cm}^{-2} \text{ d}^{-1}$  (run 1) to  $0.098 \text{ mg cm}^{-2} \text{ d}^{-1}$  (run 3) for the laboratory  
273 experiment, or even to  $0.10\text{--}0.14 \text{ mg cm}^{-2} \text{ d}^{-1}$  for the field experiment within this narrow range of pH  
274 (6.5–7.1). Laboratory dissolution rate for the highest flow rate (run 3) is similar to the field rate of weight loss  
275 at site A where faster stream flow in a rapid stream morphology would enhance the reaction process on the  
276 surface of a tablet (Table 1 and Fig. 2a). Although there are significant differences in SI<sub>c</sub> between these  
277 laboratory and field data (Fig. 7a), the ranges of pH in the output solution for all runs are slightly less than the  
278 pH of stream water at sites A and B (Fig. 7b). These facts indicate that the very high dissolution rates at sites A  
279 and B are explained by combination of stream water chemistry and high flow velocity around a tablet.

280 The results of our field and laboratory experiments support the interpretation that transport of ions around the  
281 tablet is important in dissolution of limestone in the field environment. Morse and Arvidson (2002), who  
282 summarized the results of numerous laboratory experiments on calcite dissolution, indicated that dissolution  
283 rates are controlled by transport of  $H^+$  for low pH condition ( $pH < 4$ ), and then turn to depend on surface  
284 reaction at the state of near equilibrium. For the latter case, dissolution rate decreases with increasing  $SiC$  near  
285 equilibrium state (Rickard and Sjöberg, 1983), which actually fits well with the results of Hattanji et al. (2008).  
286 Agreement of field and laboratory dissolution rates at a higher flow rates implies that transport control  
287 predominates in dissolution process at these sites even under neutral pH (6–7). Indeed, Takaya et al. (2006)  
288 conducted a series of laboratory experiments on the dissolution of limestone blocks in distilled water using a  
289 closed system, and confirmed that transport control prevails in distilled water for limestone block samples.

290

#### 291 *4.2. Implications for landscape evolution*

292 The result of the present study implies an important role of allogenic streams on landscape evolution in karst  
293 terrains. Exposed limestone will be dissolved at a high rate where unsaturated water flows rapidly such as in  
294 sites A and B. For the case of Sendaihira plateau in Abukuma Mts. (Fig. 1), stream flow originating from small  
295 basins underlain by shale enhances rapid dissolution of limestone on the eastern side of the plateau. The  
296 potential denudation rates around sites A and B can be estimated from the observed mean rate of weight loss  
297 of tablets combined with surface area and bulk density of tablets. Assuming the surface area of  $30.6 \text{ cm}^2$  and  
298 bulk density of  $2.67 \text{ g cm}^{-3}$  for each limestone tablet, estimated chemical denudation rates are equivalent to  
299  $150\text{--}187 \text{ mm ka}^{-1}$  for site A and  $71\text{--}72 \text{ mm ka}^{-1}$  for site B. These rates are much faster than the denudation  
300 rates measured at the top of karst terrain. Matsushi et al. (2010) reported denudation rates of  $20\text{--}43 \text{ mm ka}^{-1}$   
301 for pinnacles on the top of the Sendaihira plateau (Fig. 1c). Another field experiment in the Abukuma area  
302 (Matsukura et al., 2007, see Fig.1b for location) reported a slower rate of weight loss ( $0.098\% \text{ a}^{-1}$ ) in  
303 unsaturated granitic soil, which is equivalent to the denudation rate of only  $3.4 \text{ mm ka}^{-1}$ . The contrast of  
304 denudation rates on the hill top and potential rates at the eastern side of plateau should enhance the  
305 topographic contrast in time scales for landscape evolution ( $> 100 \text{ ka}$ ), although climatic change must alter  
306 hydrological and chemical conditions of stream flow, and the estimated rates must vary with time to some  
307 extent. Further discussion on the effect of allogenic stream on landscape evolution will be a future issue.

308

## 309 **5. Conclusion**

310 The present study focused on the dissolution of limestone in stream flow around a limestone plateau. In the  
311 field experiment, limestone tablets were installed in three sites (A – C) of stream from 2008 to 2011. Field rate  
312 of tablet weight loss was extremely high ( $0.11\text{--}0.14\text{ mg cm}^{-2}\text{ d}^{-1}$ ) at the high-gradient stream site A with  
313 non-carbonate sources, high ( $0.05\text{ mg cm}^{-2}\text{ d}^{-1}$ ) at the low-gradient site B with non-carbonate sources, and  
314 low ( $0.005\text{ mg cm}^{-2}\text{ d}^{-1}$ ) at the low-gradient site C with karst sources. The slowest dissolution rate was  
315 observed in the stream with a karst spring (site C) where the stream water is close to saturation to calcite ( $\text{SIc}$   
316  $\sim -0.5$ ), thus the chemical condition of stream water is the primary control on dissolution rate. The high  
317 dissolution rates at sites A and B are not only explained by chemical conditions of stream water, but also high  
318 velocity of water flow around the tablets. The laboratory dissolution rate for the case of the highest flow rate  
319 is equivalent to the highest field rate of tablet weight loss at site A. The results of our field and laboratory  
320 experiments revealed that limestone dissolves at a fast rate where continuous unsaturated water travels a  
321 relatively fast around tablet, such as in an allogenic stream. This fact implies that an allogenic stream, i.e.  
322 stream flow from non-limestone sources, has a strong impact on the local denudation of limestone and  
323 evolution of karst landscape.

324

## 325 **Acknowledgements**

326 This study is financially supported by the Science Research Fund of the JSPS (19300305) through Matsukura.  
327 The airborne LiDAR DTM provided by Kokusai Kogyo Co. Ltd. is used as the CSIS Joint Research (403).  
328 We thank Dr. Iona Dias for her technical support to improve the manuscript, and two anonymous reviewers  
329 for their constructive comments and suggestions, which improved the earlier version of the manuscript.

330

## 331 **References**

332 Crabtree, R. W., Trudgill, S. T., 1985. Chemical denudation on a Magnesian Limestone hillslope, field  
333 evidence and implications for modelling. *Earth Surface Processes and Landforms* 10, 331– 341.  
334 Dixon, J. C., Thorn, C. E., Darmody, R. G., Schlyter, P., 2001. Weathering rates of fine pebbles at the soil  
335 surface in Kärkevagge, Swedish Lapland. *Catena* 45, 273–286.

336 Ehio, M., Kanisawa, S., Taketomi, Y., 1989. Pre-Tertiary Takine Group in the central Abukuma Massif.  
 337 Bulletin of the Fukushima Museum 3, 21–37 (in Japanese).

338 Ford, D., Williams, P., 2007. Karst Hydrology and Geomorphology. Wiley, Chichester, UK.

339 Hattanji T., Yamamoto, M., Matsukura, Y., 2008. Dissolution rates of limestone tablets in a flow-through  
 340 system: A laboratory experiment. Tsukuba Geoenvironmental Sciences 4, 3–7.

341 Inkpen, R., 1995. Errors in measuring the percentage dry weight change of stone tablets. Earth Surface  
 342 Processes and Landforms 20, 783–793.

343 Jennings, J. N., 1981. Further results from limestone tablet experiments at Cooleman Plain. Australian  
 344 Geographical Studies 19, 224–227.

345 Marui, A., Hayashi, T., Kikuchi, M., Yamauchi, T., 2003. Hydrological environment of Abukuma Cave system.  
 346 Journal of Japanese Association of Hydrological Sciences 33, 71–84 (in Japanese, with English Abstr.).

347 Matsukura, Y., Hirose, T., 1999. Five-year measurement of weight loss of rock tablets due to weathering on a  
 348 forested hillslope of a humid temperate region. Engineering Geology 55, 69–76.

349 Matsukura, Y., Hattanji, T., Oguchi, C. T., Hirose, T., 2007. Ten year measurement of weight-loss of rock  
 350 tablets due to weathering in a forested hillslope of a humid temperate region. Zeitschrift für  
 351 Geomorphology N.F. 51, Supplementary Issue 1, 27–40.

352 Matsushi Y., Sasa K., Takahashi T., Sueki K., Nagashima Y., Matsukura Y., 2010. Denudation rates of  
 353 carbonate pinnacles in Japanese karst areas: estimates from cosmogenic <sup>36</sup>Cl in calcite. Nuclear  
 354 Instruments and Methods in Physics Research B 268, 1205–1208.

355 Morse, J. W. and Arvidson, R. S., 2002. The dissolution kinetics of major sedimentary carbonate minerals.  
 356 Earth Science Reviews 58, 51–84.

357 Parkhurst, D. L., Appelo, C. A. J., 1999. User's guide to PHREEQC (Version 2) – A computer program for  
 358 speciation, batch-reaction, one-dimensional transport, and inverse geochemical calculations. U. S.  
 359 Geological Survey Water-Resources Investigations Report 99–4259, Denver, CO.

360 Plan, L., 2005. Factors controlling carbonate dissolution rates quantified in a field test in the Austrian Alps.  
 361 Geomorphology, 68, 201–212.

362 Rickard, D. T., Sjöberg, E. L., 1983. Mixed kinetic control of calcite dissolution rates. American Journal of  
 363 Science 283, 815–830.

364 Smith, D. I., Atkinson, T.C., 1976. Process, landforms and climate in limestone regions. In: Derbyshire, E. D.  
 365 (Ed.), *Geomorphology and Climate*, Wiley, New York, pp. 367–409.  
 366 Suzuki, M., Takaya, Y., Matsukura, Y., 2000. Dissolution experiment of limestone tablets. *Bulletin of the*  
 367 *Terrestrial Environment Research Center, University of Tsukuba* 1, 19–26 (in Japanese).  
 368 Takaya, Y., Hirose, T., Aoki, H., Matsukura, Y., 2006. Dissolution characteristics of limestone in laboratory  
 369 experiments. *Journal of Geography (Japan)* 115, 136–148 (in Japanese, with English Abstr.).  
 370 Thorn, C. E., Darmody, R. G., Dixon, J. C., Schlyter, P., 2002. Weathering rates of buried machine-polished  
 371 rock disks, Kärkevagge, Swedish Lapland. *Earth Surface Processes and Landforms* 27, 831–845.  
 372 Thorn, C.E. Dixon, J. C., Darmody, R. G., Allen, C. E., 2006. Ten years (1994–2004) of ‘potential’ weathering  
 373 in Kärkevagge, Swedish Lapland. *Earth Surface Processes and Landforms* 31, 992–1002.  
 374 Trudgill, S. T., 1977. Problems in the estimation of short-term variations in limestone erosion processes. *Earth*  
 375 *Surface Processes* 2, 251–256.  
 376 Trudgill, S. T., Crabtree, R. W., Ferguson, R. I., Ball, J., Gent, R., 1994. Ten year remeasurement of chemical  
 377 denudation on a Magnesian Limestone hillslope. *Earth Surface Processes and Landforms* 19, 109–114.  
 378 Urushibara-Yoshino, K., Kashima, N., Enomoto, H., Kuramoto, T., Miotoke, F. D., Nakahodo, T., Higa,  
 379 M., 1999. Secular change and regional differences of limestone solution rates in Japan. *Journal of*  
 380 *Geography (Japan)* 108, 45–58 (in Japanese, with English Abstr.).  
 381 White, W. B., 1988. *Geomorphology and Hydrology of Karst Terrains*. Oxford University Press, New York.  
 382 Williams, P.W., 1983. The role of the subcutaneous zone in karst hydrology. *Journal of Hydrology* 61, 45–67.  
 383 Yokoyama, T., Matsukura, Y., 2006. Field and laboratory experiments on weathering rates of granodiorite:  
 384 Separation of chemical and physical processes. *Geology* 34, 809–812.  
 385 Yoshimura, K., Fujikawa, M., Ishida, M., Kurisaki, K., Aizawa, J., 2009. Cave wall erosion near the entrance  
 386 to Akiyoshi-do Cave, Yamaguchi, Southwestern Japan. *Journal of Speleological Society of Japan* 34,  
 387 38–46.  
 388  
 389

390    *Captions*

391    Fig.1    Location and geologic map of the study area (A, B) and relief shading map using LiDAR DTM with  
392    2 m resolution around the study sites (C). Contour interval of Fig. 1b is 20 m.    In Fig. 1c, the white broken  
393    line shows the margin of limestone exposure, and the broken lines with black arrows indicate the connection  
394    between dolines and caves proven by Marui et al. (2003).

395

396    Fig. 2    Stream sites for the field experiment. Direction of stream flow is indicated with an arrow. A mesh  
397    bag with two limestone tablets is indicated with a circle for each site.

398

399    Fig. 3    Surface of the limestone tablets installed at sites A, B and C after the experiment and surface of a  
400    non-weathered polished limestone (D). All photographs were taken with magnification of 20×.

401

402    Fig. 4    Temporal variation of pH (A) and saturation index with respect to calcite (SI<sub>c</sub>, B) for stream water.  
403    Daily rainfall was recorded at Ono-niimachi nearby the investigation sites.

404

405    Fig. 5    A flow-through apparatus using a peristaltic pump for the laboratory experiment. Distilled water in  
406    an input solution bottle is infused into a 60-mL reaction bottle, in which one limestone tablet is placed.

407

408    Fig. 6    Effects of water flow rate on dissolution rate of calcite or rate of weight loss for limestone tablet.  
409    The uncertainty is not shown if it is smaller than the size of plot itself.

410

411    Fig. 7    Comparison of field and laboratory weathering experiments. (A) Relationship between saturation  
412    index for calcite (SI<sub>c</sub>) and weathering rates, (B) relationship between pH and weathering rates. Data from  
413    Hattanji et al. (2008) shows the results of a similar laboratory experiment at a flow rate of 63 mL d<sup>-1</sup> using  
414    limestone tablets under different initial solutions.

415



416 Table 1 Hyrdological and geomorphic conditions for the sites of field weathering experiment

	Site A	Site B	Site C
Lithology of source area	shale	shale, partly limestone	limestone
Local channel gradient [ $\text{m m}^{-1}$ ]	0.15	0.08	0.04
Drainage area [ $\text{km}^2$ ]	0.062	0.321	0.071*
Stream width at base flow [m]	0.3	1.0	0.3
Discharge at base flow [ $\text{cm}^3 \text{s}^{-1}$ ]	$390 \pm 40$	$4900 \pm 1400$	$86 \pm 43$
Estimated water flux [ $\text{cm s}^{-1}$ ]	$6.5 \pm 4.0$	$4.9 \pm 2.2$	$0.3 \pm 0.2$
Channel morphology	rapid	pool	pool

417 \*the estimated drainage area for site C is a reference value based on surface topography because groundwater  
 418 flow system of this karst plateau is unknown.

419 Table 2 Weight loss of tablets in the field experiment

Tablet No.	Site A		Site B		Site C	
	17	18	8	23	9	21
Measured weight loss [g]*	3.530	4.366	1.672	1.666	0.133	0.151
Net weight loss [g]*	3.523	4.359	1.665	1.659	0.128	0.145
Mean rate of weight loss [ $\text{mg cm}^{-2} \text{d}^{-1}$ ]**	0.109	0.137	0.052	0.053	0.005	0.006
Annual weight loss ratio [ $\% \text{a}^{-1}$ ]***	4.47	5.72	2.14	2.17	0.19	0.23

420 \*Uncertainty is 0.004 g for measured weight loss, and 0.005 g for net weight loss.

421 \*\*Relative errors are 2.3% for tablets in sites A and B, 4.2–4.6% for site C.

422 \*\*\*Relative errors are 0.7% for all tablets.

423 Table 3 Chemical conditions of stream water in the field experiment. The data is an average of 21  
 424 measurements, and the standard deviation of measurements is shown as an error.

	Site A	Site B	Site C
pH	$6.96 \pm 0.35$	$7.14 \pm 0.37$	$7.40 \pm 0.33$
alkalinity [meq kg <sup>-1</sup> ]	$0.32 \pm 0.04$	$0.33 \pm 0.04$	$2.01 \pm 0.24$
Ca <sup>2+</sup> conc. [mg kg <sup>-1</sup> ]	$3.2 \pm 0.7$	$3.3 \pm 0.6$	$42.2 \pm 5.8$
SIc	$-2.8 \pm 0.4$	$-2.5 \pm 0.4$	$-0.48 \pm 0.36$

425

426 Table 4 Dissolution rate and rate of weight loss for limestone tablets in the laboratory experiment

	Run #1	Run #2	Run #3
Flow rate [mL d <sup>-1</sup> ]	98 ± 2	553 ± 21	4510 ± 150
Tablet weight before the run [g]	26.266	24.874	25.151
Tablet weight after the run [g]	26.239	24.821	25.062
Weight loss of tablet [mg]	27 ± 5	53 ± 5	89 ± 5
Mean rate of weight loss [mg cm <sup>-2</sup> d <sup>-1</sup> ]*	0.037 ± 0.002	0.075 ± 0.004	0.124 ± 0.007
Dissolution rate of calcite [mg cm <sup>-2</sup> d <sup>-1</sup> ]**	0.018	0.056 ± 0.001	0.098 ± 0.002
Average pH for output water	6.96 ± 0.12	6.85 ± 0.14	6.47 ± 0.16
Average SIc for output water***	-3.1 ± 0.2	-3.8 (+0.3, -0.5)	-5.0 (+0.4, -1.4)
SIc in the reaction bottle at the end***	-0.61 ± 0.2	-1.6 ± 0.2	-3.5 (+0.4, -1.9)

427 \*mean rate of weight loss during the 24-day experiment.

428 \*\*dissolution rate calculated from the temporal increase of  $W_n$ . The error is not shown if it is < 0.001.

429 \*\*\*The asymmetric uncertainties shown in the parentheses are originated from errors of low alkalinity < 0.1  
 430 meq kg<sup>-1</sup>.

431

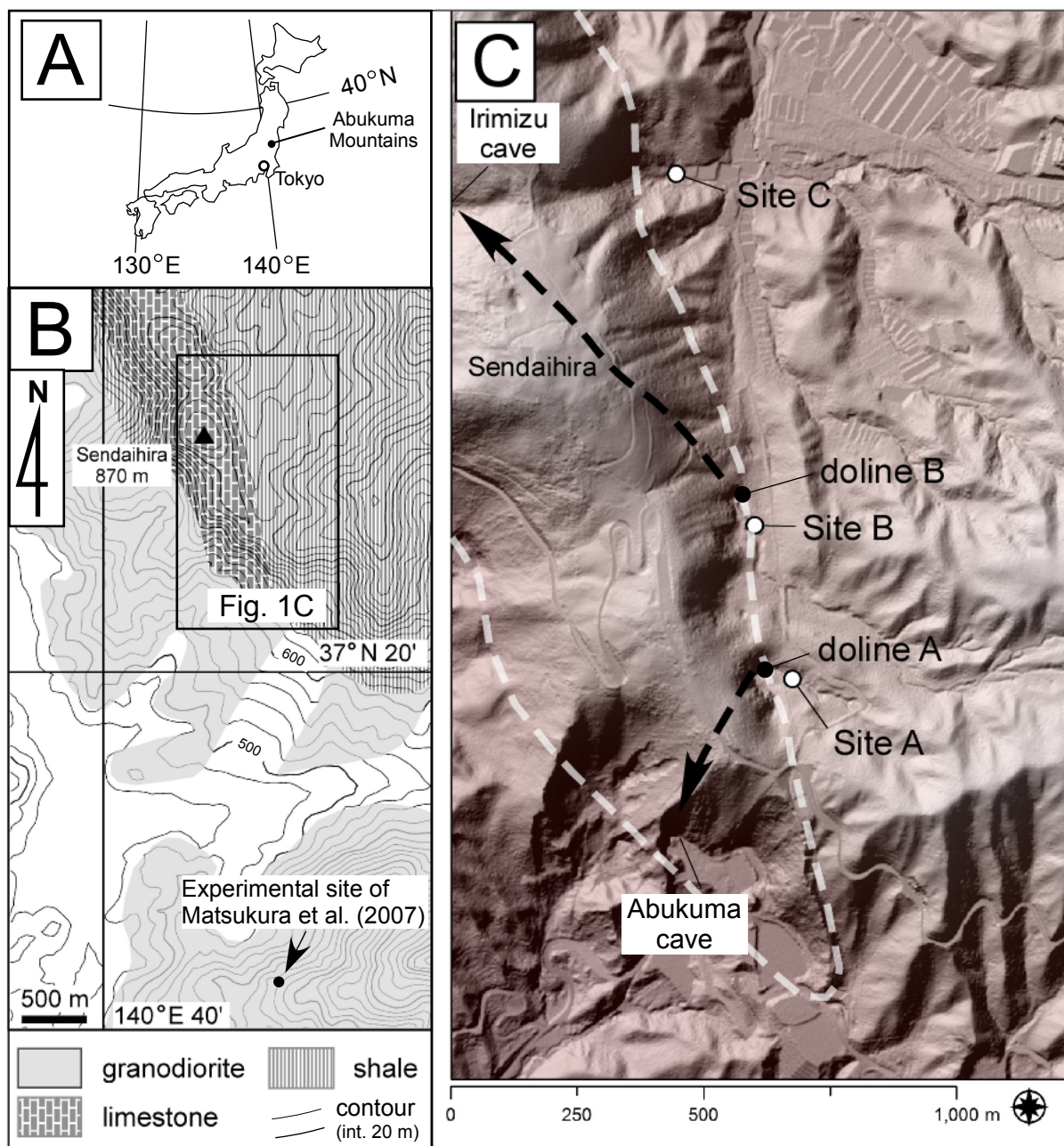


Figure 1

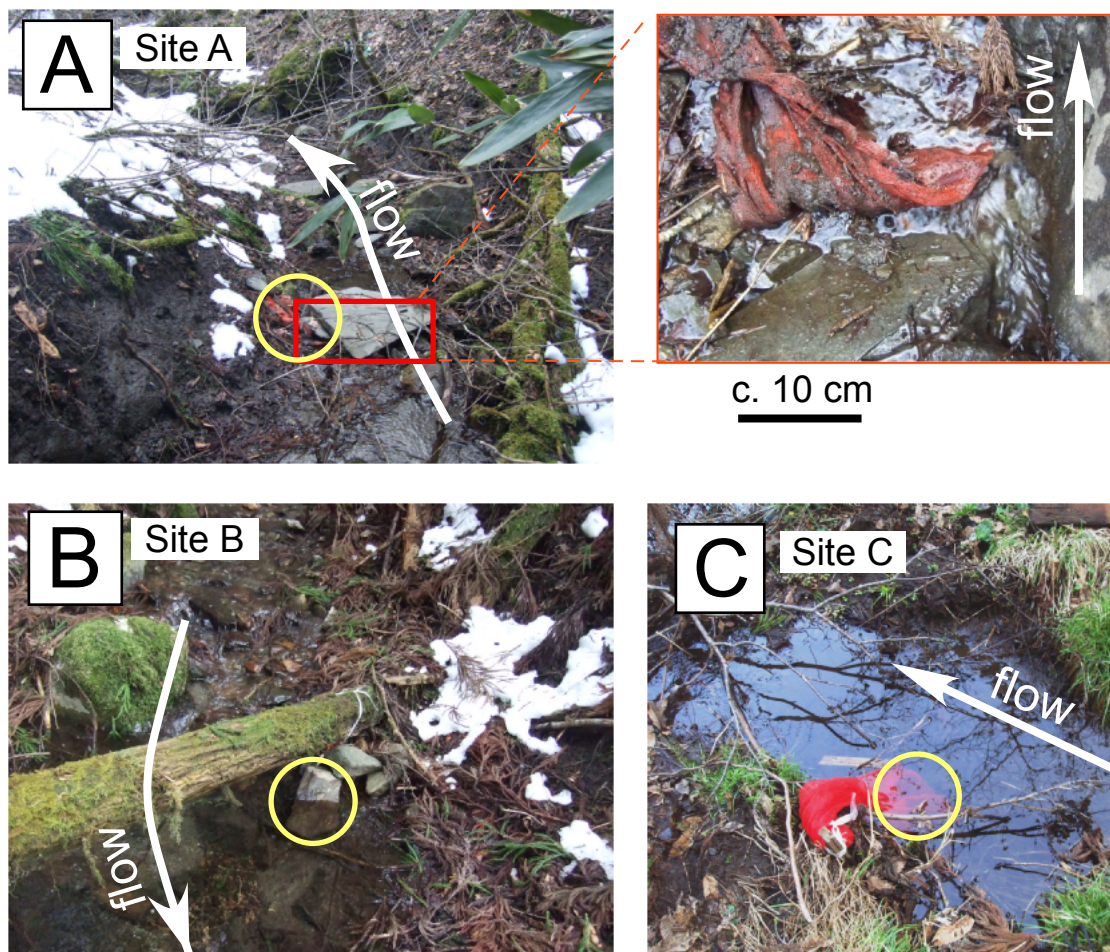


Figure 2



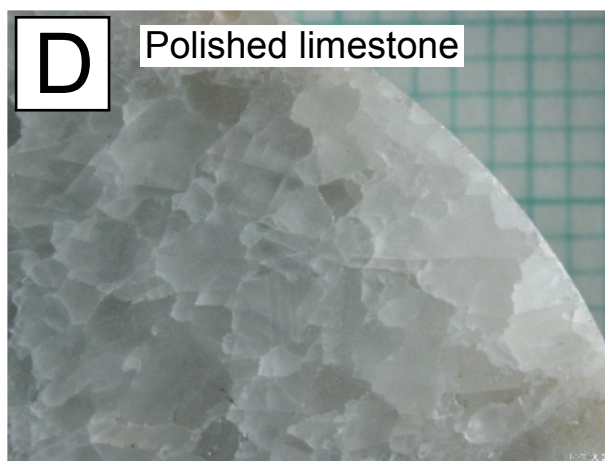


Figure 3

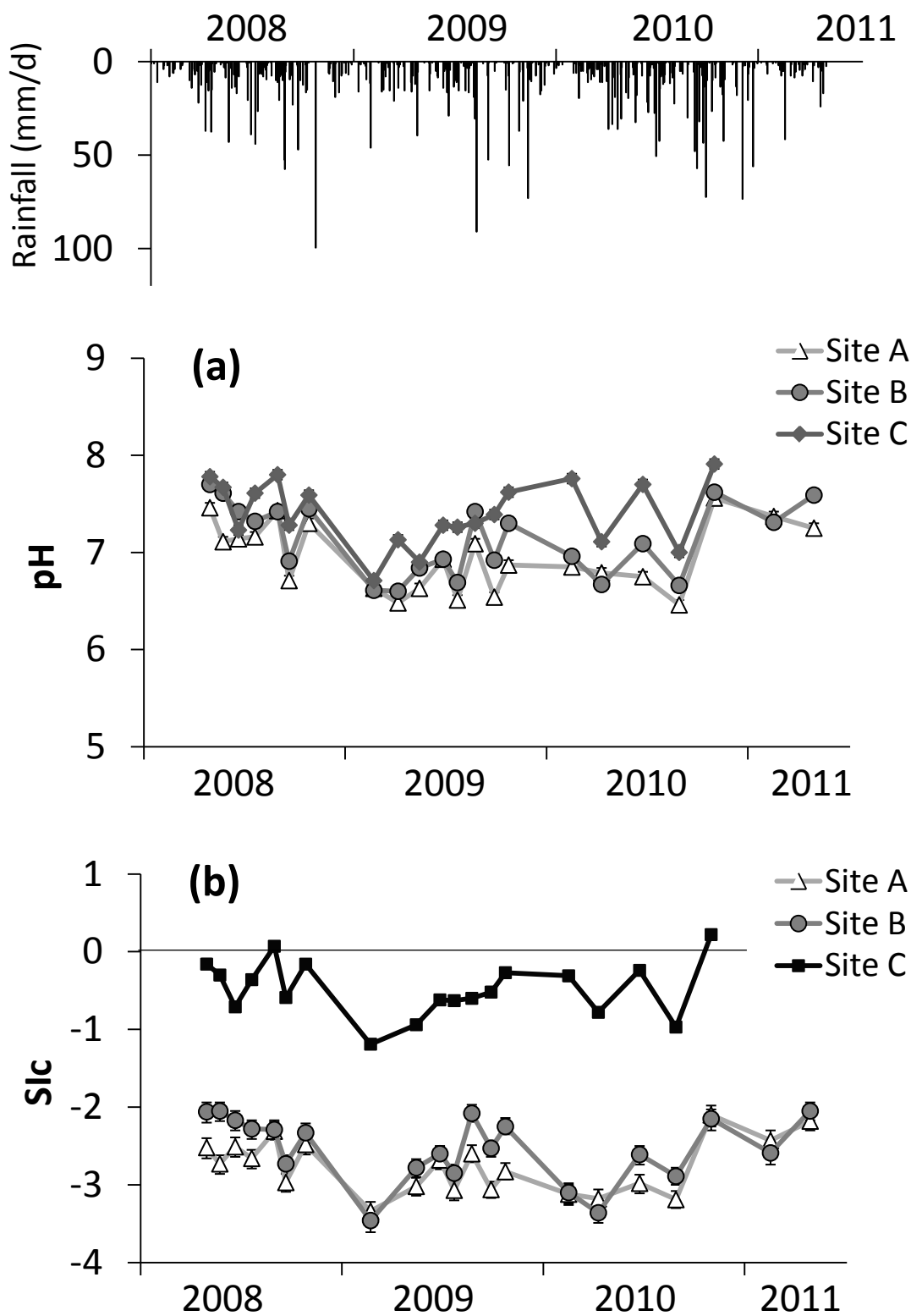


Figure 4



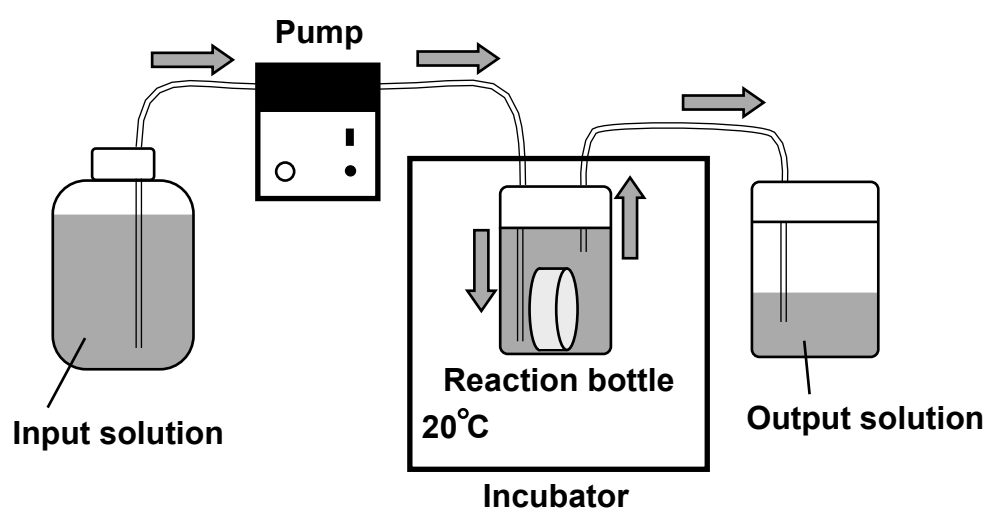


Figure 5

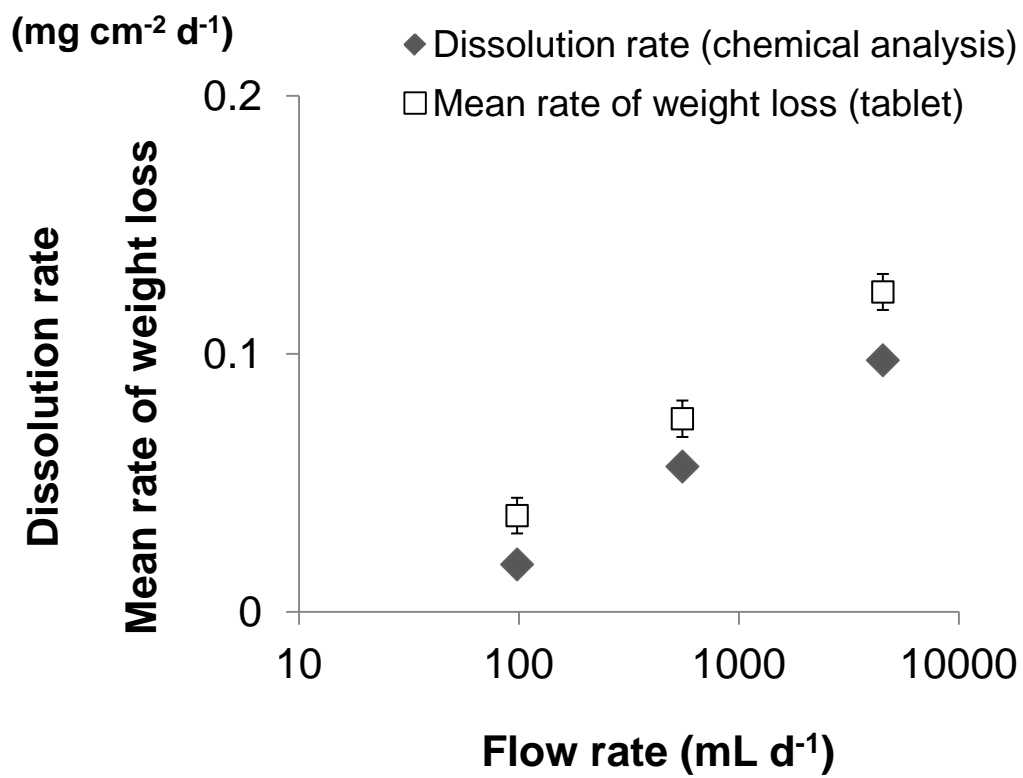


Figure 6

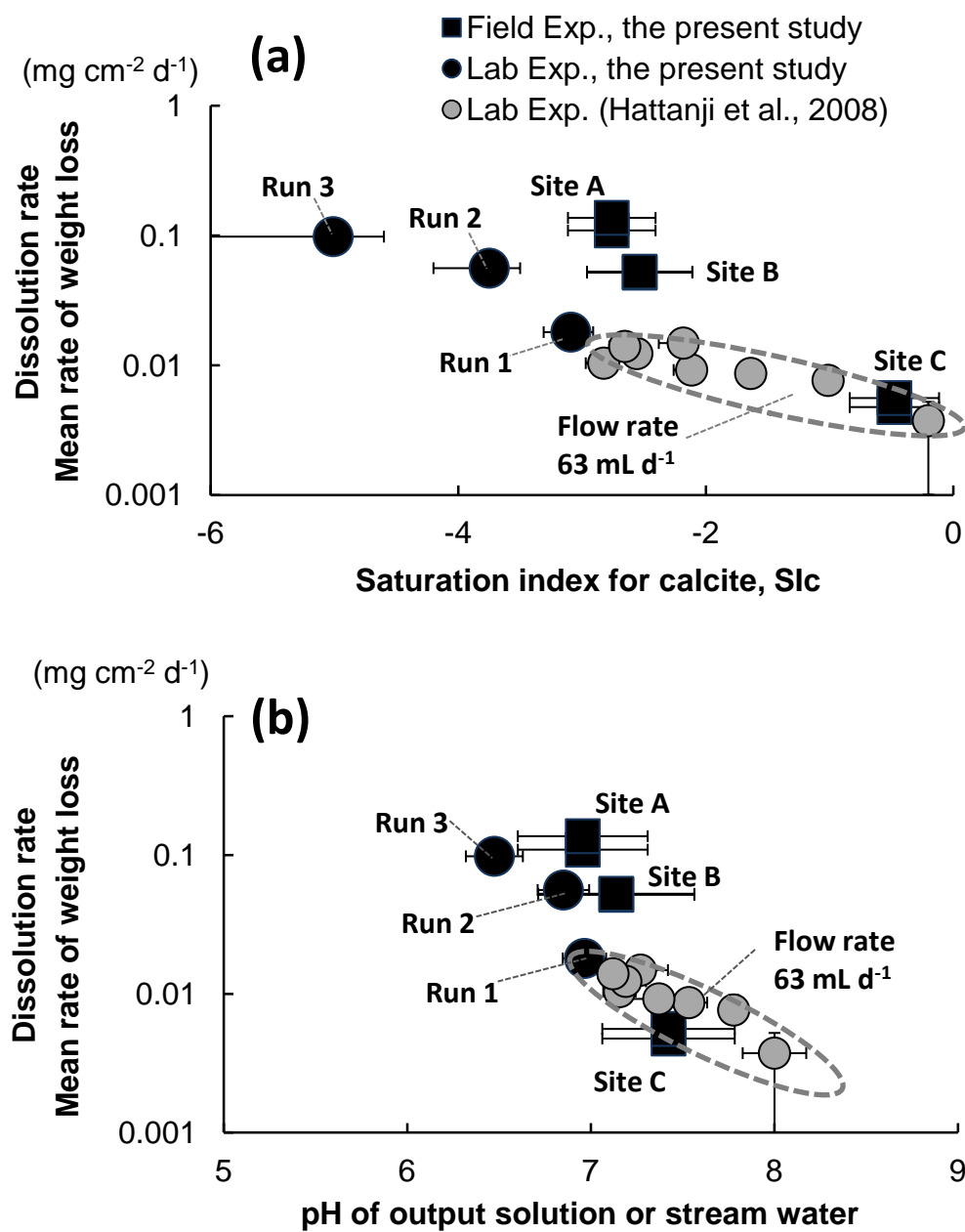


Figure 7